

# ADS-Based Guidelines for Thinned Planar Arrays

Giacomo Oliveri, *Member, IEEE*, Luca Manica, *Graduate Student Member, IEEE*, and Andrea Massa, *Member, IEEE*

**Abstract**—We propose an analytical technique based on almost difference sets (ADSs) for thinning planar arrays with well controlled sidelobes. The method allows one to synthesize bidimensional arrangements with peak sidelobe levels (PSLs) predictable and deducible from the knowledge of the array aperture, the filling factor, and the autocorrelation function of the ADS at hand. The numerical validation, concerned with both small and very large apertures, points out that the expected PSL values are significantly below those of random arrays and comparable with those from different sets (DSs) although obtainable in a wider range of configurations.

**Index Terms**—Almost difference sets, array antennas, planar arrays, sidelobe level control, thinned arrays.

## I. INTRODUCTION

ANTENNA arrays for radar tracking, remote sensing, biomedical imaging, satellite and ground communications have often to support three-dimensional scanning with a suitable beam pattern shape in the whole angular region [1]. Towards this end, planar arrays have to be used and large apertures are necessary to provide satisfactory angular resolutions along both azimuth and elevation [1]. On the other hand, the inter-element spacing should not exceed half-wavelength to avoid the presence of grating lobes [1]. These requirements usually result in very inefficient, heavy, and expensive solutions consisting of planar geometries with several thousands close elements.

In order to reduce the number of elements while keeping the radiation properties of the original structures, thinning techniques have been successfully introduced [2]. Designing thinned planar arrays is an important research topic since decades (see [2]–[8] and the references cited therein). As a matter of fact, a suitable thinning allows one to reduce the array costs, its weight, and the power consumption. However, it causes the loss of the control of the peak sidelobe level (PSL) [6] to be properly counteracted. To this end, several techniques have been proposed in order to fully exploit the advantages of thinned arrangements while minimizing their drawbacks. First attempts have been conceived to require low computational resources (see [9, Table I]), but they have provided no significant

improvements when compared with random placements [2], [9] extensively employed in practice [2].

More recently, the availability of large computational resources has justified the use of optimization techniques such as dynamic programming [10], [11], genetic algorithms [5], [7], [8], [12], simulated annealing [13]–[17], and particle swarm optimizers [18]. Thinned arrays synthesized with optimization tools turn out to be very effective [7], [8], [11], [14], even though it is not possible to *a-priori* estimate the expected performances for a given array aperture and thinning factor [6]. Furthermore, computational and convergence issues make the application of stochastic optimizers difficult and expensive when dealing with 1D large apertures [6] and, even more, when planar arrangements are considered.

In order to overcome such drawbacks, an alternative approach for thinning large arrays has been introduced (see [4] for the linear case and [6], [9], [20]–[22] for both linear and planar cases). Such an approach relies on the exploitation of binary sequences derived from difference sets (DSs), which exhibit a two-level autocorrelation function [4], or from DSs extensions [19]–[21]. Besides their analytic nature and the arising inexpensive generation, DS-based thinned arrays have several interesting properties. They are deterministically designed and present predictable [6] and low PSLs (3 dB and 1.5 dB below random arrays for the linear case and the planar one, respectively). However, only a limited number of DS sequences exist and the whole set of aperture sizes and thinning values [6], [23] cannot be dealt with.

The problem of obtaining sub-optimal sequences (in terms of autocorrelation levels) has been recently addressed in information theory and “close” sequences to DSs have been looked for. Almost difference sets (ADSs) [24]–[26] are a wide class of binary sequences with *three-valued* autocorrelations [24]–[26]. They represent the closest sets to DSs [24]–[26] (three-levels vs. two-levels) and can be defined in a much broader set of aperture sizes and thinning values with respect to DSs [27]. Furthermore large repositories of explicit sequences are now available (e.g., [28]). They have been determined by numerically implementing the generating rules coming from the information-theory/combinatorial-mathematics literature (e.g., [26]).

As regards 1D geometries, the sidelobe characteristics of ADS-based arrays have been analyzed in [27] and good performances have been predicted and numerically verified dealing with both small and large apertures. Because of these results, its deterministic nature, and preliminary examples of planar arrays based on a subset ADSs with peculiar power patterns features (see [19]–[21] and the references therein for more details), an ADS-based technique seems to be a good candidate for thinning planar arrangements of radiating elements and it

Manuscript received June 25, 2009; revised November 13, 2009; accepted December 16, 2009. Date of publication March 29, 2010; date of current version June 03, 2010. This work was supported in part by the Italian National Project: Wireless multiplatform mimo active access networks for QoS-demanding multimedia Delivery (WORLD), under Grant 2007R989S.

The authors are with the Department of Information Engineering and Computer Science, University of Trento, Povo 38050 Trento-Italy (e-mail: giacomo.oliveri@disi.unitn.it; luca.manica@disi.unitn.it; andrea.massa@ing.unitn.it).

Color versions of one or more of the figures in this paper are available online at <http://ieeexplore.ieee.org>.

Digital Object Identifier 10.1109/TAP.2010.2046858

will be presented in this paper. More specifically, the objective is not to define the “optimal” thinning method, but rather to provide a simple and reliable technique which guarantees to the designer predictable performances to be taken into account during the feasibility study. Towards this end, the PSL behavior of ADS-based planar arrays will be analytically investigated and, for the first time to the best of the author’s knowledge, different bounds will be provided by considering the whole and in a general fashion the whole class of 2D ADSs. It should be pointed out that, despite the linear case [27] where the Blahut’s theorem [27] has been applied, a different mathematical analysis is here necessary. Unlike the mathematical approach in [27] and [6], the PSL bounds are then derived starting from an innovative formulation based on the 2D discrete Fourier transform and related theorems, which allows a compact and straightforward analytical formulation.

The paper is organized as follows. After a short overview on ADSs (Section II), a set of suitable bounds of the PSL are analytically determined in Section III. Section IV provides a selected set of numerical results aimed at validating the obtained PSL estimators as well as comparing the ADS performances with both random techniques and state-of-the-art optimization approaches. The exploitation of directive elements is also considered in order to point out the flexibility of the ADS thinning theory. Finally, some conclusions are drawn (Section V).

## II. TWO-DIMENSIONAL ALMOST DIFFERENCE SETS

With reference to the 2D problem, let us define a  $(PQ, K, \Lambda, t)$ -almost difference set as a  $K$ -subset  $\underline{D} = \{\mathbf{d}_k \in \underline{G}, k = 0, \dots, K-1\}$  of the Abelian group  $\underline{G}$  of order  $PQ$  ( $\underline{G} \triangleq \mathbb{Z}^P \otimes \mathbb{Z}^Q$ ,<sup>1</sup>  $P$  and  $Q$  being chosen according the Kronecker decomposition theorem [29]) for which the multiset

$$\underline{M} = \{\mathbf{m}_j = (\mathbf{d}_h - \mathbf{d}_\ell), \mathbf{d}_\ell \neq \mathbf{d}_h; j = 0, \dots, K(K-1)-1\}$$

contains  $t$  nonzero elements of  $\underline{G}$  each exactly  $\Lambda$  times and the remaining  $PQ - 1 - t$  nonzero elements each exactly  $\Lambda + 1$  times [26]. Therefore, an ADS satisfies the following existence condition [25], [26]:

$$K(K-1) = t\Lambda + (PQ - 1 - t)(\Lambda + 1) \quad (1)$$

where  $K \geq \Lambda + 1$ ,  $0 \leq K \leq PQ$ , and  $0 \leq t \leq PQ - 1$ . Moreover, it is worth noticing that DSs are ADSs for which  $t = PQ - 1$  or  $t = 0$  [26].

If  $\underline{D}$  is a  $(PQ, K, \Lambda, t)$  - ADS, then it is possible to derive a two dimensional binary sequence  $\underline{W} = \{w(p, q) = 1(0) \text{ if } (p, q) \in (\notin)\underline{D}; p = 0, \dots, P-1, q = 0, \dots, Q-1\}$

<sup>1</sup>The symbol  $\otimes$  stands for the *direct sum* of the abelian groups  $\mathbb{Z}^P$  and  $\mathbb{Z}^Q$ , that is  $\underline{G} = \{\mathbf{g}_i = (j, h), i = 0, \dots, PQ-1, j = 0, \dots, P-1, h = 0, \dots, Q-1\}$  and  $\underline{G}$  is equipped with the component-wise operations derived from  $\mathbb{Z}^P$  and  $\mathbb{Z}^Q$ , that is  $\mathbf{g}_1 + \mathbf{g}_2 = ((j_1 + j_2)_{\text{mod } P}, (h_1 + h_2)_{\text{mod } Q})$ .

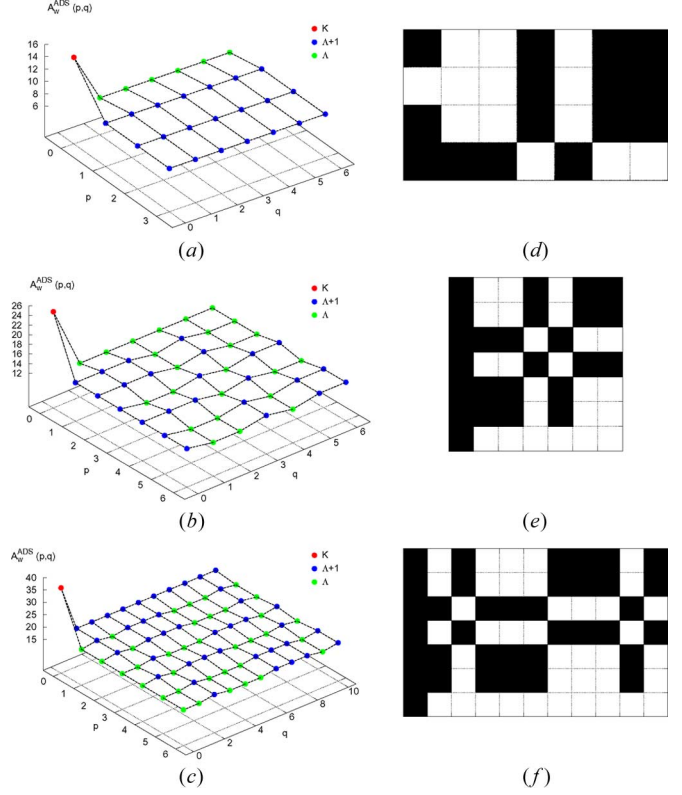


Fig. 1. Autocorrelation functions and associated binary sequences of the ADSs in Table I: (a), (d)  $\underline{D}_1$ , (b), (e)  $\underline{D}_2$ , and (c), (f)  $\underline{D}_3$ .

whose 2D periodic autocorrelation function [6]  $A_w(p, q)$  ( $p \in [0, P-1]$ ,  $q \in [0, Q-1]$  being its periodicity) is a three-level function [24], [26]

$$A_w^{\text{ADS}}(p, q) = (K - \Lambda)\delta(p, q) + \Lambda + \sum_{r=1}^{N-1-t} \delta(p - l_{r,1}, q - l_{r,2}) \quad (2)$$

where  $K \geq \Lambda + 1$ ,  $\delta(p, q) = 1$  if  $p = q = 0$  and  $\delta(p, q) = 0$  otherwise, and  $(l_{r,1}, l_{r,2}) \triangleq \mathbf{l}_r$  is an element of the set  $\underline{L} = \{\mathbf{l}_r \in \mathbb{Z}^P \otimes \mathbb{Z}^Q, r = 1, \dots, N-1-t\}$ . For descriptive purposes, let us consider the ADSs in Table I [26], [28]. The plots of  $\underline{W}$  and of the three-level function  $A_w^{\text{ADS}}(p, q)$  in correspondence with  $\underline{D}_i$  ( $i = 1, 2, 3$ ) are shown in Fig. 1.

As regards the closeness of the ADS to the DS sequences, likewise 1D arrangements, the bidimensional autocorrelation function of a  $(PQ, K, \Lambda, t)$  - ADS differs from  $A_w^{\text{DS}}(p, q) = K\delta(p, q) + \Lambda$  [6] by a unity in only  $PQ - 1 - t$  points [24], [26] [(2)]. Moreover, the ADS autocorrelation function still remains unaltered after cyclic shifts of the reference sequence [24], [26] since if  $\underline{D}$  is an ADS, then

$$\underline{D}^{(\sigma_x, \sigma_y)} = \left\{ \left( (p + \sigma_x)_{\text{mod } P}, (q + \sigma_y)_{\text{mod } Q} \right) \mid (p, q) \in \underline{D}, \sigma_x, \sigma_y \in \mathbb{Z} \right\} \quad (3)$$

is still an ADS. As a consequence, starting from a  $(PQ, K, \Lambda, t)$  - ADS, it is always possible to build  $P \times Q$  different  $(PQ, K, \Lambda, t)$  - ADSs by applying cyclic shifts to its elements.

Concerning the ADS generation, several theorems have already been proposed in information theory and combinatorial mathematics (e.g., see [26] and references therein). Analogously, the explicit forms of many others ADSs have been determined and they are now available in [28]. Furthermore, suitable techniques/theorems for completing the whole set of theoretically admissible ADS sequences are still a work-in-progress [24]–[26] in related fields of research non-properly concerned with electromagnetics/antenna-theory and out-of-the-scope of this paper.

### III. ADS-BASED PLANAR ARRAYS—MATHEMATICAL FORMULATION

Let us consider a planar array of  $P \times Q$  elements located, according to the binary sequence  $\underline{\mathbf{W}}$ , on a bidimensional lattice of points spaced by  $d_x$  and  $d_y$  wavelengths along the  $x$  and  $y$  directions, respectively. The array factor of such an elements arrangement turns out to be [1], [6]

$$\begin{aligned} AF\{\underline{\mathbf{W}}\} &\triangleq W_{AF}(u, v) \\ &= \sum_{p=0}^{P-1} \sum_{q=0}^{Q-1} w(p, q) \exp[2\pi j(pd_x u + qd_y v)] \end{aligned} \quad (4)$$

where  $u = \sin(\theta) \cos(\phi)$  and  $v = \sin(\theta) \sin(\phi)$ . Moreover,  $W_{AF}(u, v)$  can be also expressed in terms of the 2D discrete time Fourier transform (DTFT) of the sequence  $\underline{\mathbf{W}}$ ,

$$\text{DTFT}\{\underline{\mathbf{W}}\} \triangleq \mathbb{T}(\alpha, \beta) = \sum_{p=0}^{P-1} \sum_{q=0}^{Q-1} w(p, q) \exp[-j(p\alpha + q\beta)] \quad (5)$$

as follows:

$$W_{AF}(u, v) = \mathbb{T}(-2\pi d_x u, -2\pi d_y v). \quad (6)$$

Furthermore, by applying the sampling theorem [30] to the function  $\mathbb{T}(\alpha, \beta)$ ,

$$\mathbb{T}(\alpha, \beta) = \sum_{k=0}^{P-1} \sum_{l=0}^{Q-1} \mathbb{F}(k, l) \mathbb{S}_P\left(\frac{\alpha}{2} - \frac{k\pi}{P}\right) \mathbb{S}_Q\left(\frac{\beta}{2} - \frac{l\pi}{Q}\right) \quad (7)$$

$\mathbb{F}$  being 2D (DFT) of the sequence  $\underline{\mathbf{W}}$  ( $\text{DFT}\{\underline{\mathbf{W}}\} \triangleq \mathbb{F}(k, l) = \sum_{p=0}^{P-1} \sum_{q=0}^{Q-1} w(p, q) \exp[-2\pi j((pk/P) + (ql/Q))]$ ) and  $\mathbb{S}_R(x) \triangleq \sin(Rx)/R \sin(x)$ , it results that

$$\begin{aligned} W_{AF}(u, v) &= \sum_{k=0}^{P-1} \sum_{l=0}^{Q-1} \mathbb{F}(k, l) \\ &\quad \times \mathbb{S}_P\left(\pi d_x u + \frac{k\pi}{P}\right) \mathbb{S}_Q\left(\pi d_y v + \frac{l\pi}{Q}\right). \end{aligned} \quad (8)$$

Such a relationship states that the samples of the array factor at  $u = k/d_x P$ ,  $v = l/d_y Q$  are equal to the values of the DFT of the weighting sequence  $\underline{\mathbf{W}}$  in  $(k, l)$

$$W_{AF}\left(-\frac{k}{d_x P}, -\frac{l}{d_y Q}\right) = \mathbb{F}(k, l). \quad (9)$$

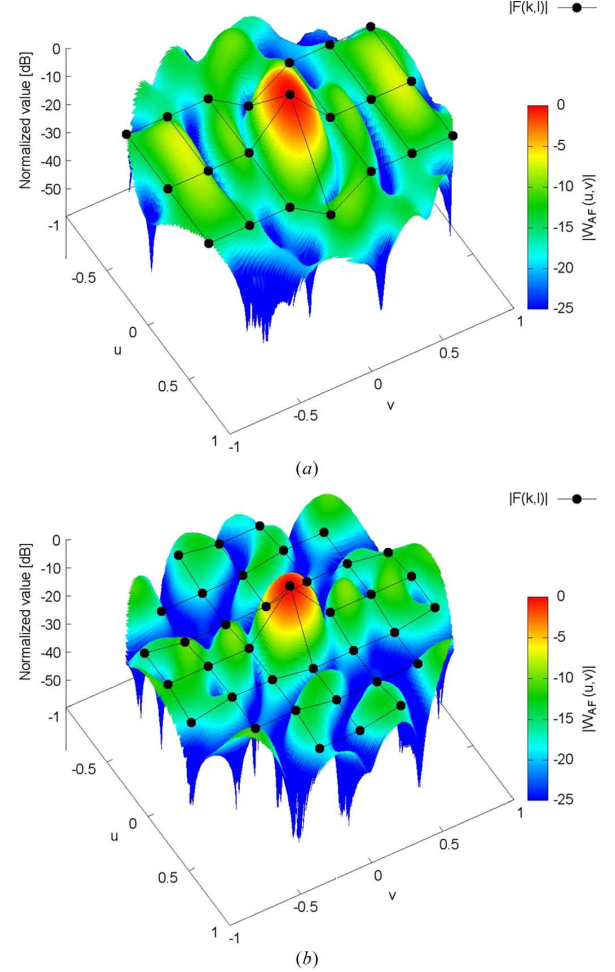


Fig. 2. Plot of the normalized array factor derived from  $\underline{\mathbf{D}}_i = \underline{\mathbf{D}}_i^{(\sigma_x=0, \sigma_y=0)}$  and associated  $|\mathbb{F}(k, l)|$  values: (a)  $i = 1$  and (b)  $i = 2$ .

For illustrative purposes, Fig. 2 shows the plot of the array factor ( $d_x = d_y = 1/2$ ) and the samples of the DFT of  $\underline{\mathbf{W}}$  in correspondence with the set  $\underline{\mathbf{D}}_1$  [Fig. 2(a)] and the set  $\underline{\mathbf{D}}_2$  [Fig. 2(b)].

As regards the peak sidelobe level (PSL), it is defined as

$$\text{PSL}\{\underline{\mathbf{D}}^{(\sigma_x, \sigma_y)}\} \triangleq \frac{\max_{(u,v) \notin R} |W_{AF}^{(\sigma_x, \sigma_y)}(u, v)|^2}{|W_{AF}^{(\sigma_x, \sigma_y)}(0, 0)|^2} \quad (10)$$

where  $W_{AF}^{(\sigma_x, \sigma_y)}(u, v)$  is the array factor coming from the shifted set  $\underline{\mathbf{D}}^{(\sigma_x, \sigma_y)}$  and  $R$  is the main-lobe region of extension

$$\begin{aligned} R &\triangleq \{(u, v) \in [-1, 1] \times [-1, 1] : u^2 + v^2 \leq 1, \\ &\quad uv \leq \frac{K}{4PQd_x d_y \max_{(k,l) \in \mathcal{H}_0} |\mathbb{F}(k, l)|}\} \end{aligned} \quad (11)$$

(see Appendix) with  $\mathcal{H}_0 \triangleq \underline{\mathbf{G}} \setminus (0, 0)$ .<sup>2</sup>

<sup>2</sup>The notation  $\underline{\mathbf{G}} \setminus (0, 0)$  indicates the set of elements of the Abelian group  $\underline{\mathbf{G}}$  without the null element,  $(0, 0)$ .

TABLE I  
EXAMPLES OF ADSs AND DESCRIPTIVE PARAMETERS

ADS	$P$	$Q$	$K$	$\Lambda$	$t$	$\nu \triangleq \frac{K}{PQ}$	$\eta \triangleq \frac{t}{PQ-1}$	Reference
$\underline{\mathbf{D}}_1$	4	7	15	7	6	$\approx 0.5357$	$\approx 0.22$	[26]
$\underline{\mathbf{D}}_2$	7	7	25	12	24	$\approx 0.5102$	0.5	[26]
$\underline{\mathbf{D}}_3$	7	11	37	17	36	$\approx 0.4805$	$\approx 0.4736$	[26]
$\underline{\mathbf{D}}_4$	23	23	265	132	264	$\approx 0.5$	0.5	[28]
$\underline{\mathbf{D}}_5$	73	73	2665	1332	2664	$\approx 0.5$	0.5	[28]
$\underline{\mathbf{D}}_6$	199	199	19801	9900	19800	$\approx 0.5$	0.5	[28]

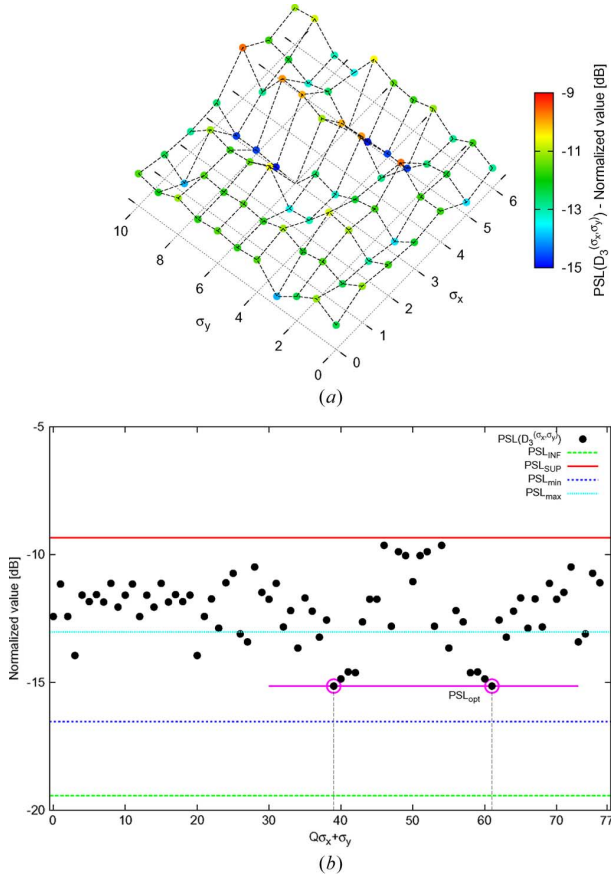


Fig. 3. PSL values of the ADS-based planar arrays derived from the sequences  $\underline{\mathbf{D}}_3^{(\sigma_x, \sigma_y)}$ ,  $\sigma_x = 0, \dots, P-1$ ,  $\sigma_y = 0, \dots, Q-1$  (a) and PSL bounds (b). Number of elements:  $P \times Q = 7 \times 11$ —aperture size:  $3\lambda \times 5\lambda$ .

By substituting (8) in (10),

$$\text{PSL} \left\{ \underline{\mathbf{D}}^{(\sigma_x, \sigma_y)} \right\} = \frac{1}{K^2} \max_{(u,v) \notin R} \left| \sum_{k=0}^{P-1} \sum_{l=0}^{Q-1} \mathbb{F}^{(\sigma_x, \sigma_y)}(k, l) \times \mathbb{S}_P \left( \pi d_x u + \frac{k\pi}{P} \right) \mathbb{S}_Q \left( \pi d_y v + \frac{l\pi}{Q} \right) \right|^2 \quad (12)$$

is obtained, since  $\mathbb{F}^{(\sigma_x, \sigma_y)}(0, 0) = \sum_{p=0}^{P-1} \sum_{q=0}^{Q-1} w^{(\sigma_x, \sigma_y)}(p, q) = K$ ,  $\underline{\mathbf{W}}^{(\sigma_x, \sigma_y)} = \{w^{(\sigma_x, \sigma_y)}(p, q); p = 0, \dots, P-1; q = 0, \dots, Q-1\}$  being the two-dimensional sequence derived from  $\underline{\mathbf{D}}^{(\sigma_x, \sigma_y)}$ . As it can be noticed, the PSL of an ADS-based array is a function of the coefficients  $\mathbb{F}^{(\sigma_x, \sigma_y)}(k, l)$ . Unfortunately, since these coefficients cannot be expressed in closed-form (but their values are available when the generating ADS is known) and, unlike DSs, depends on the indexes  $k$  and  $l$ , it is not possible to

provide a PSL threshold as for DSs-based planar arrays [6]. Nevertheless, the following set of inequalities holds true for sufficiently large values of  $P$  and  $Q$  (Appendix)

$$\text{PSL}_{\text{INF}} \leq \text{PSL}_{\text{min}} \leq \text{PSL}^{\text{opt}} \{ \underline{\mathbf{D}} \} \leq \text{PSL}_{\text{max}} \leq \text{PSL}_{\text{SUP}} \quad (13)$$

where  $\text{PSL}^{\text{opt}} \{ \underline{\mathbf{D}} \} = \min_{(\sigma_x, \sigma_y)} [\text{PSL} \{ \underline{\mathbf{D}}^{(\sigma_x, \sigma_y)} \}]$ ,  $\text{PSL}_{\text{min}} = (\Xi \{ \underline{\mathbf{D}} \} / K^2) [0.5 + 0.8 \log_{10}(PQ)]$ ,  $\text{PSL}_{\text{max}} = \Omega \{ \underline{\mathbf{D}} \} E \{ \Gamma_{PQ}^{\text{opt}} \} / K^2$ ,  $\text{PSL}_{\text{INF}} = (K - \Lambda - \sqrt{(t+1)(PQ-1-t)/(PQ-1)}) / K^2$ ,  $\text{PSL}_{\text{SUP}} = (K - \Lambda + \sqrt{(t+1)(PQ-1-t)/(PQ-1)}) E \{ \Gamma_{PQ}^{\text{opt}} \} / K^2$ ,  $\Omega \{ \underline{\mathbf{D}} \} = \max_{(k,l) \in \mathcal{H}_0} |\mathbb{F}^{(\sigma_x, \sigma_y)}(k, l)|^2$ ,  $\Xi \{ \underline{\mathbf{D}} \} = \min_{(k,l) \in \mathcal{H}_0} |\mathbb{F}^{(\sigma_x, \sigma_y)}(k, l)|^2$ , and  $E \{ \Gamma_{PQ}^{\text{opt}} \} \approx -0.1 + 1.5 \log_{10}(PQ)$ .

It is now worth pointing out that  $\text{PSL}_{\text{min}}$  and  $\text{PSL}_{\text{max}}$  can be evaluated only once the ADS sequence is exactly known, since the knowledge of the term  $|\mathbb{F}^{(\sigma_x, \sigma_y)}(k, l)|^2$  is required, while the bounds  $\text{PSL}_{\text{INF}}$  and  $\text{PSL}_{\text{SUP}}$  can be *a-priori* determined starting for the knowledge of the characteristic parameters describing the ADS (i.e.,  $P$ ,  $Q$ ,  $K$ ,  $\Lambda$ , and  $t$ ).

For a preliminary validation of such an estimate criterion, let us refer to the planar array generated by  $\underline{\mathbf{D}}_3$  in Table I. As expected, the PSL of the set  $\underline{\mathbf{D}}_3^{(\sigma_x, \sigma_y)}$  depends on the values of  $\sigma_x$  and  $\sigma_y$  [Fig. 3(a)] and different shift values give the same optimal PSL,  $\text{PSL}_{\text{opt}}$ , whose value lies into the range of confidence defined in (13) [Fig. 3(b)]. The multiplicity of the optimal solutions indicates that less than  $P \times Q$  evaluations are actually needed to identify the optimal ADS-based planar array. This is a negligible computational cost compared to the burden required by stochastic optimization techniques to determine a thinned arrangement on the same aperture. As regards the simple steps required to design an ADS-based array they consist in: (a) selecting the desired aperture size  $\hat{P} \times \hat{Q}$  and thinning factor  $\hat{\nu}$  for the designed array (on the basis of the application constraints); (b) evaluating the expected PSL for the final ADS array by means of (13); (c) if the expected PSL complies with the application requirements, selecting from [27] (or other repositories) an ADS  $\underline{\mathbf{D}}$  with size and thinning factor as close as possible to  $\hat{P} \times \hat{Q}$  and  $\hat{\nu}$ ; (d) deriving the optimal array by applying cyclic shifts to  $\underline{\mathbf{D}}$  and evaluating the arising PSL.

#### IV. NUMERICAL ANALYSIS

In this section, the results of a numerical assessment are described and discussed to point out potentialities and limitations of the ADS-based approach proposed as a suitable tool for predicting the performance of an effective set of planar thinned arrays. For comparison purposes, random arrangements [3], [6] are considered as reference since, likewise ADS arrays, their



performances can be *a-priori* estimated. More in detail, the estimator of the normalized peak sidelobe level of planar random arrays (RND) turns out to be [3]

$$\text{PSL}_{\text{RND}} = 1/K \left\{ -\ln \left( 1 - \beta \frac{\lambda^2}{\pi^2 x_0 y_0 (P-1)(Q-1)} \right) + 1 - 2 \left[ \ln \left( 1 - \beta \frac{\lambda^2}{\pi^2 x_0 y_0 (P-1)(Q-1)} \right) \right]^{-1} \right\} \quad (14)$$

where  $\beta$  is the probability or confidence level that no sidelobe exceeds the  $\text{PSL}_{\text{RND}}$  value. Moreover, random lattice planar arrays (RNL), whose elements are located on a uniformly-spaced lattice of points over the aperture, exhibit the following PSL [6]

$$\text{PSL}_{\text{RNL}} = \text{PSL}_{\text{RND}} \times (1 - \nu) \quad (15)$$

where  $\nu = K/PQ$  is the thinning factor (such an expression, which is valid for  $\nu$  not close to one, can be obtained by trivial extension to the 2D case of [6, Eq. (25)]).

The first numerical example deals with the analysis of the PSL bounds (13) versus  $\eta \triangleq t/(PQ - 1)$  for different apertures and when  $\nu = 0.5$  (Fig. 4).

As expected (Section II), the upper bound of PSL tends to  $\text{PSL}_{\text{DS}}$  when  $\eta = 1$  and  $\eta = 0$  ( $PQ \rightarrow \infty$ ) and its value,  $\text{PSL}_{\text{SUP}}$ , is always below  $\text{PSL}_{\text{RND}}$  and  $\text{PSL}_{\text{RNL}}$  except for a small set of  $\eta$  values close to  $\eta = 0.5$  and large apertures ( $PQ \geq 10^6$ ). As a matter of fact, whatever the array dimension, the worst performances verify in correspondence with  $\eta = 0.5$ . Therefore, such an index value will be analyzed in the following to provide “worst-case” indications on ADS-based thinning.

Fig. 5(b) shows the behaviors of the ADS bounds versus the aperture dimension ( $\nu = \eta = 0.5$ ). Since ADS are here available [28],  $\text{PSL}_{\text{opt}}$ ,  $\text{PSL}_{\text{min}}$ , and  $\text{PSL}_{\text{max}}$  are reported, as well. As it can be noticed, these plots confirm that  $\text{PSL}_{\text{SUP}}$  usually overestimates the actual peak sidelobe of the ADS array and that  $\text{PSL}_{\text{opt}}$  is always well below the values exhibited by random families. For completeness, the remaining of Fig. 5 gives an indication on the estimated behavior of ADS arrays in correspondence with different thinning percentages [ $\nu = 0.4$ —Fig. 5(a),  $\nu = 0.5$ —Fig. 5(b),  $\nu = 0.6$ —Fig. 5(c)] for which ADSs are not still available. As regards the confidence range  $\Delta_{\text{ADS}}$ , defined as

$$\Delta_{\text{ADS}} \triangleq \frac{\text{PSL}_{\text{SUP}}}{\text{PSL}_{\text{INF}}} \quad (16)$$

it slightly increases with  $PQ$  and shows a limited dependence on the aperture dimension ( $\sim 4$  dB in  $10^2 \leq PQ \leq 10^6$ ) (Fig. 6). Moreover,  $\Delta_{\text{ADS}}(\nu) = \Delta_{\text{ADS}}(1 - \nu)$  and the minimum value of  $\Delta_{\text{ADS}}$  verifies for  $\nu = 0.5$  as it can be analytically derived.

Concerning available ADSs with  $\nu \neq 0.5$ , Fig. 7 shows the behavior of the  $\text{PSL}_{\text{opt}}$  (and related bounds) of the array generated from the sequence  $\underline{\mathbf{D}}_3$  ( $\eta = 0.473$  and  $\nu = 0.485$ ) whose power pattern and elements arrangement are given in Fig. 7(b) and Fig. 7(c), respectively. Despite the small aperture ( $3\lambda \times 5\lambda$ ),  $\text{PSL}_{\text{opt}}$  still lies in the range of values estimated by (13) [Fig. 7(a)] and it appears to be significantly below the random estimates and comparable with the DS value at  $\eta = 1$ . It is also interesting to notice that the reference array derived

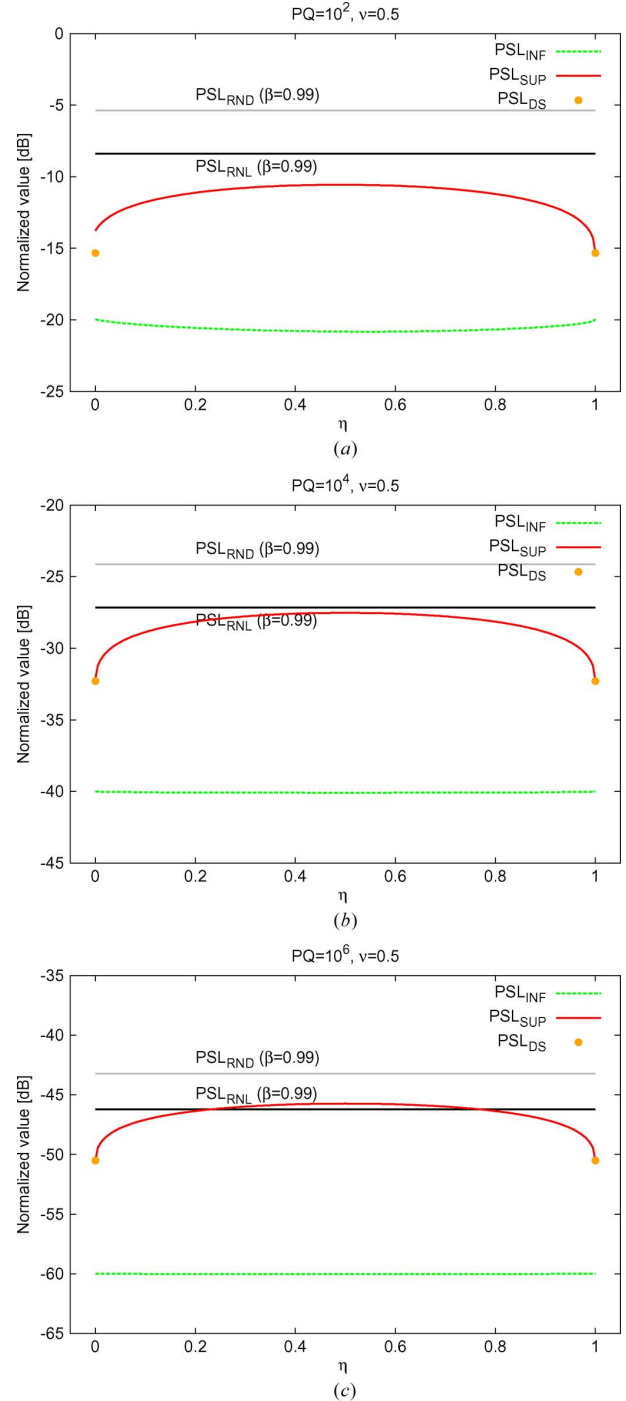


Fig. 4. Numerical Validation. Plots of the PSL bounds of ADS-based planar arrays, the estimator of the PSL of random (RND) and random lattice (RNL) arrays, and values of the PSL of DS-based finite arrays versus  $\eta$  when  $\nu = 0.5$  and (a)  $PQ = 10^2$ , (b)  $PQ = 10^4$ , (c)  $PQ = 10^6$ .

from  $\underline{\mathbf{D}}_3$  allows one to determine several shifted array configurations with  $\text{PSL}\{\underline{\mathbf{D}}_3^{(\sigma_x, \sigma_y)}\} \leq \text{PSL}_{\text{SUP}}$  [Fig. 3(b)] as well as multiple arrays with  $\text{PSL}\{\underline{\mathbf{D}}_3^{(\sigma_x, \sigma_y)}\} \leq \text{PSL}_{\text{max}}$ .

Such a feature is not only limited to  $\underline{\mathbf{D}}_3$ , but it is a common property of ADS-based arrays as confirmed by the examples in Figs. 8–10 and concerned with larger apertures.

Furthermore, it should be pointed out that more than one cyclic shift of the reference ADS sequence  $\underline{\mathbf{D}}_i$  ( $i = 4, \dots, 7$ )

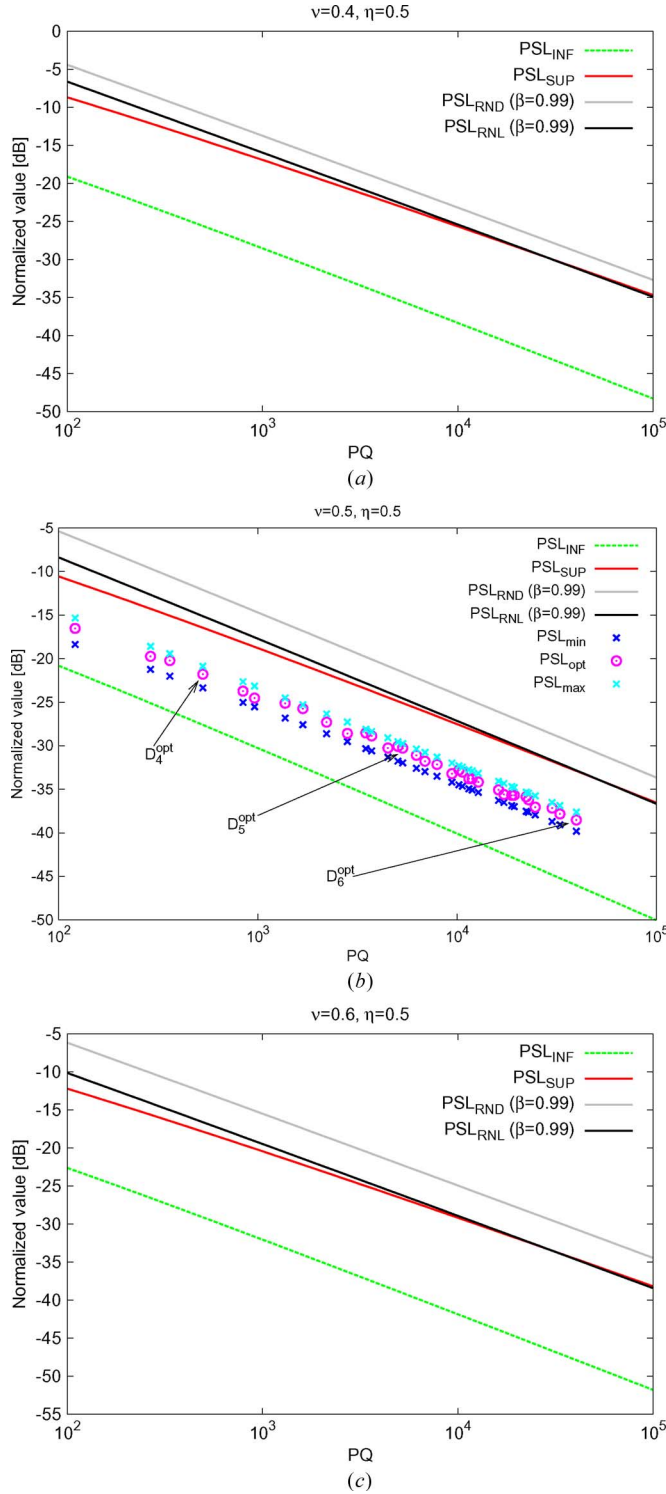


Fig. 5. Numerical Validation. Plots of the PSL bounds of ADS-based planar arrays and the estimators of the PSL of random (RND) and random lattice (RNL) arrays versus the array aperture,  $PQ$ , when  $\eta = 0.5$  and (a)  $\nu = 0.4$ , (b)  $\nu = 0.5$ , (c)  $\nu = 0.6$ .

gives an array pattern with  $\text{PSL}\{\mathbf{D}_i^{(\sigma_x, \sigma_y)}\} = \text{PSL}_{\text{opt}}$  [Figs. 3(b), 8(a), 9(a), 10(a)]. Such considerations highlight that: (a) also through an exhaustive search, less than  $P \times Q$  evaluations are actually needed to identify the optimal ADS-based planar array; (b) a very limited number of evaluations is enough

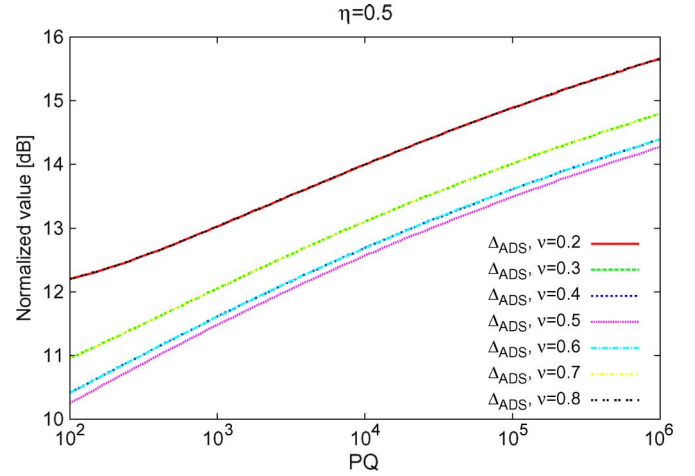


Fig. 6. Numerical Validation. Plots of  $\Delta_{\text{ADS}}$  versus the array aperture,  $PQ$ , when  $\eta = 0.5$  and in correspondence with different thinning values  $\nu \in [0, 1]$ .

to synthesize an ADS array with a PSL value below that from random/random lattice distributions.

As far as the radiation patterns are concerned, Figs. 7(b) and 8(c)–10(c) allow one to point out a further interesting property of ADS planar arrays. Unlike DSs, where  $|\mathbf{F}(k, l)|$  is a two-valued function [6], the unequal magnitudes of the samples of  $|\mathbf{F}(k, l)|$  (Fig. 2) lead to a non-uniform behavior of the array pattern outside the mainlobe region with some non-negligible variations of the sidelobes [see Figs. 7(b) and 8(c)–10(c)]. This can be exploited as an additional degree of freedom to be used in antenna synthesis. One efficient way to do that is to consider directive elements.

As an example, let us consider the planar arrays synthesized from  $\mathbf{D}_4$  with isotropic or directive elements (e.g.,  $\lambda/2$  dipoles along the  $y$  axis). Fig. 11(a) gives the PSL values for different shifts of the reference set. As it can be observed, the value of  $\text{PSL}_{\text{opt}}$  reduces ( $\text{PSL}_{\text{opt}}^{\text{dir}} = -23.66$  dB vs.  $\text{PSL}_{\text{opt}} = -21.79$  dB) thanks to the use of directive elements and, more interestingly, the optimal shift for the directive array is not equal to that with isotropic elements ( $\sigma_{x,\text{opt}}^{\text{dir}} = 5$ ,  $\sigma_{y,\text{opt}}^{\text{dir}} = 20$  vs.  $\sigma_{x,\text{opt}} = 7$ ,  $\sigma_{y,\text{opt}} = 5$ ). This is due to the following. One has to determine the shift generating the lowest lobes in the whole sidelobe region when dealing with the “isotropic” array [Fig. 11(b)]. Otherwise, the use of directive elements suggests to choose the  $\sigma_x$  and  $\sigma_y$  values with lowest sidelobes only near the mainlobe region [Fig. 11(c)] since the element factor “erases” the highest sidelobes far from the mainlobe region in the resulting antenna pattern [Fig. 11(d)].

The last section of the numerical validation is aimed at giving some indications on the performance of the ADS arrays versus those coming from state-of-the-art thinning techniques based on stochastic optimizers [5], [7], [18]. Since ADSs are not still available in correspondence with the thinning percentage of the test cases under analysis, the comparison cannot be considered fully fair, but it can be useful to suggest some guidelines for a fast and reliable choice of the most suitable synthesis procedure as well as on the achievable PSL results.

Fig. 12 shows the PSL of the thinned arrays optimized with the methods in [5], [Fig. 12(a)], [7], [Fig. 12(b)], and [18],

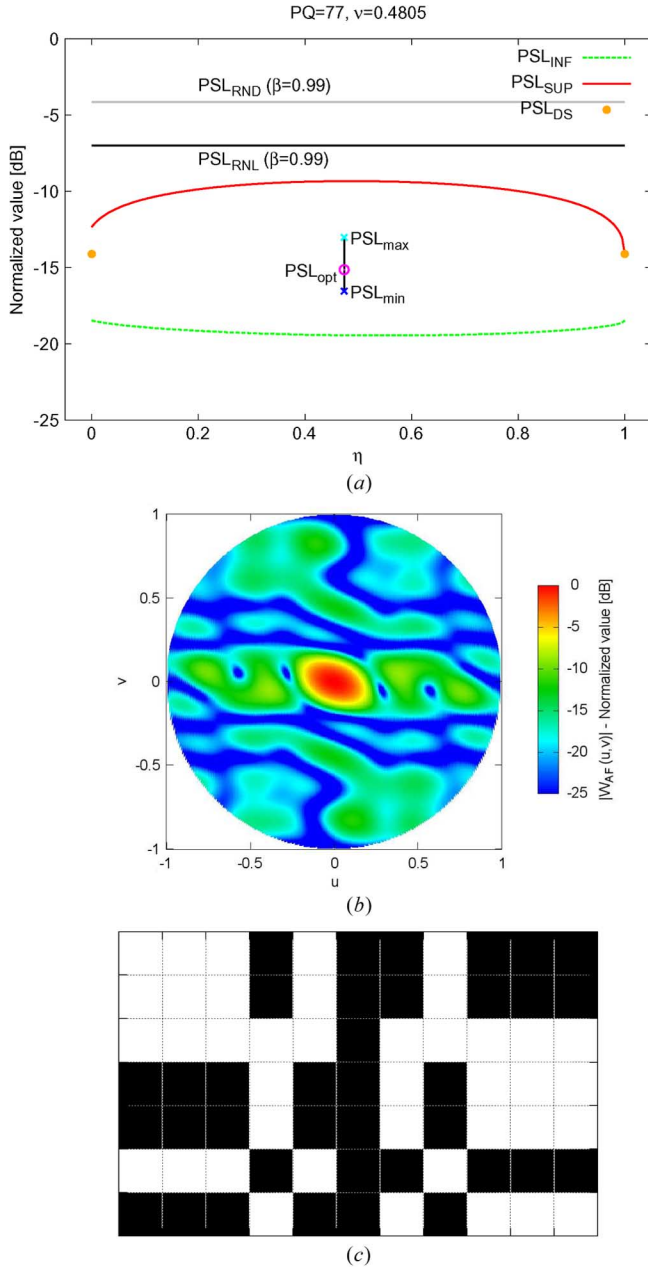


Fig. 7. Numerical Validation—Planar Array  $\underline{D}_3^{opt}$  [Number of elements:  $P \times Q = 7 \times 11$ —aperture size:  $3\lambda \times 5\lambda$ ]. Plots of the PSL bounds versus  $\eta$  [ $PQ = 77, \nu = 0.4805$ ] (a). Plot of the normalized array factor (b) generated from the  $\underline{D}_3^{opt}$ -based array arrangement (c).

[Fig. 12(c)], respectively, along with the PSL bounds derived for the corresponding ADS-based arrays (i.e., only the values of  $PSL_{SUP}$  and  $PSL_{INF}$  since the ADS sequences, although theoretically existing, have not been yet determined). As it can be noticed, ADS-based arrays compare favorably in terms of PSL with global optimized designs since, even in the worst case (i.e.,  $\eta = 0.5$ ),  $PSL_{INF} < PSL^{gl} \leq PSL_{SUP}$ .

## V. CONCLUSION

In this paper, ADSs have been considered for the design of thinned planar arrays. The research work is aimed at identifying the descriptive parameters of the ADS-based thinning technique as well as their effect on the array performances.

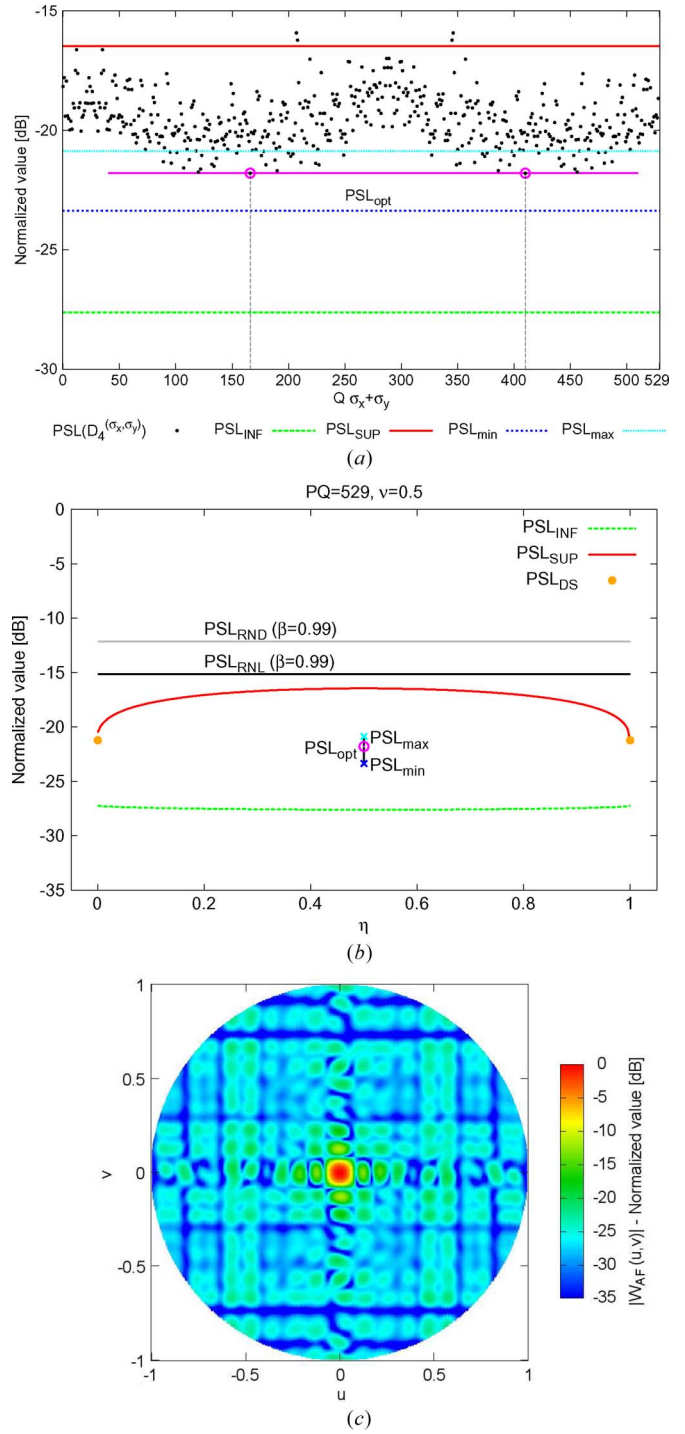


Fig. 8. Numerical Validation—Planar Array  $\underline{D}_4^{opt}$  [Number of elements:  $P \times Q = 23 \times 23$ —aperture size:  $11\lambda \times 11\lambda$ ]. PSL values of the ADS-based arrays derived from the sequences  $\underline{D}_4^{(\sigma_x, \sigma_y)}$ ,  $\sigma_x = 0, \dots, P-1, \sigma_y = 0, \dots, Q-1$  (a). Plots of the PSL bounds versus (b)  $\eta$  [ $PQ = 529, \nu = 0.5$ ]. Plot of the normalized array factor (c) generated from the  $\underline{D}_4^{opt}$ -based array arrangement.

Likewise the linear case [27], the objective of this study is to analytically define a “term of comparison” to help the array designer in identifying the synthesis approach allowing the optimal trade-off between computational resources and the achievable result in terms of PSL level. Towards this purpose, the performances of planar ADS-based arrays have been investigated and suitable bounds for the PSL have been determined



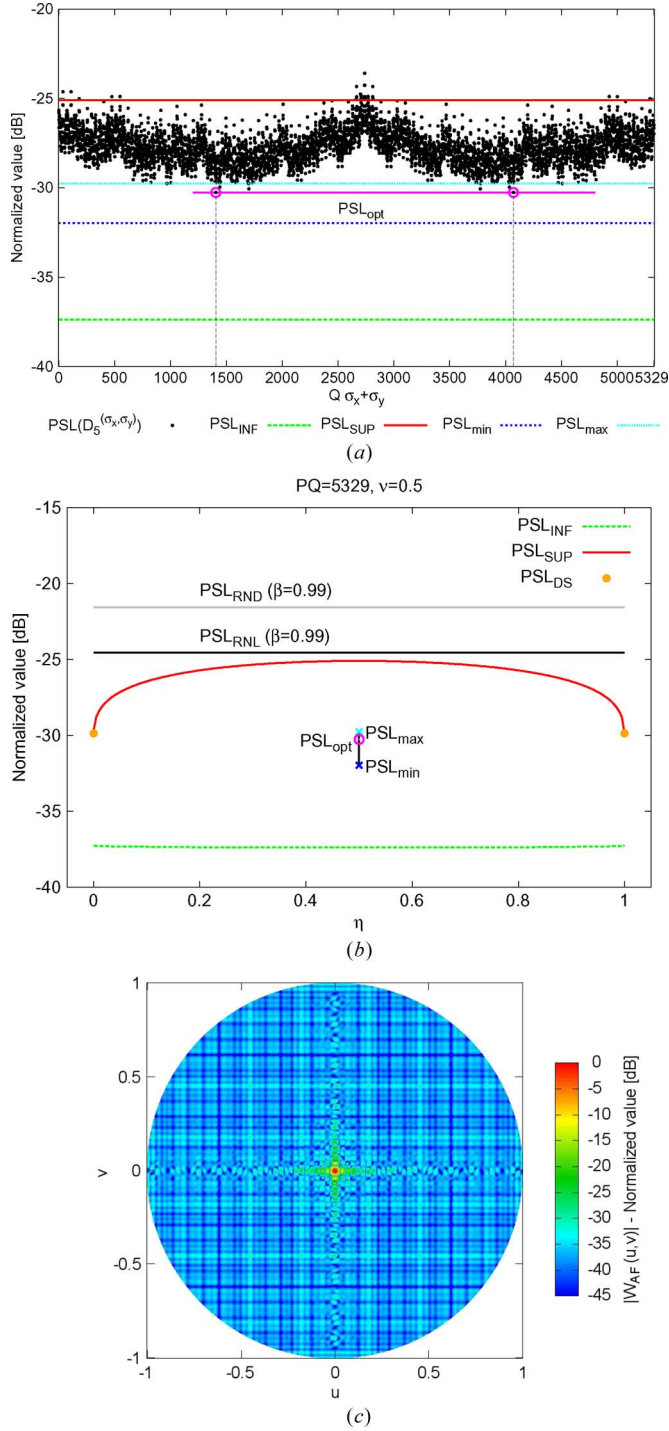


Fig. 9. Numerical Validation—Planar Array  $\mathbf{D}_5^{\text{opt}}$  [Number of elements:  $P \times Q = 73 \times 73$ —aperture size:  $36\lambda \times 36\lambda$ ]. PSL values of the ADS-based arrays derived from the sequences  $\mathbf{D}_5^{(\sigma_x, \sigma_y)}$ ,  $\sigma_x = 0, \dots, P-1$ ,  $\sigma_y = 0, \dots, Q-1$  (a). Plots of the PSL bounds versus (b)  $\eta$  [ $PQ = 5329$ ,  $\nu = 0.5$ ]. Plot of the normalized array factor (c) generated from the  $\mathbf{D}_5^{\text{opt}}$ -based array arrangement.

thanks to a new formulation based on the properties of the two-dimensional DFT. Such an analysis has been validated by means of a large set of numerical experiments also aimed at comparing the predicted ADS performances with those of random distributions or stochastically optimized arrays.

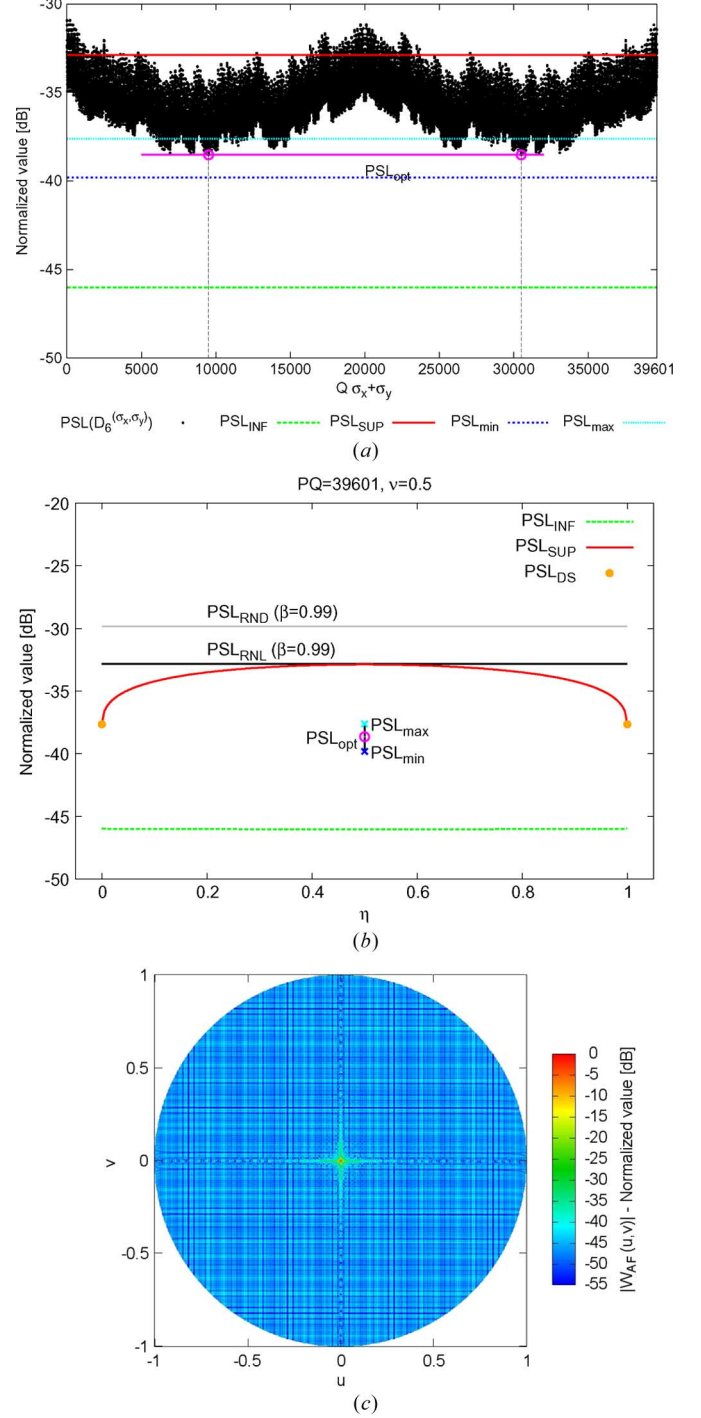


Fig. 10. Numerical Validation—Planar Array  $\mathbf{D}_6^{\text{opt}}$  [Number of elements:  $P \times Q = 199 \times 199$ —aperture size:  $99\lambda \times 99\lambda$ ]. PSL values of the ADS-based arrays derived from the sequences  $\mathbf{D}_6^{(\sigma_x, \sigma_y)}$ ,  $\sigma_x = 0, \dots, P-1$ ,  $\sigma_y = 0, \dots, Q-1$  (a). Plots of the PSL bounds versus (b)  $\eta$  [ $PQ = 39601$ ,  $\nu = 0.5$ ]. Plot of the normalized array factor (c) generated from the  $\mathbf{D}_6^{\text{opt}}$ -based array arrangement.

The obtained results have pointed out the following features of the ADS thinning technique:

- the PSL of the synthesized pattern is *a-priori* known when the ADS sequence is available in an explicit form, while suitable bounds are predictable, otherwise;



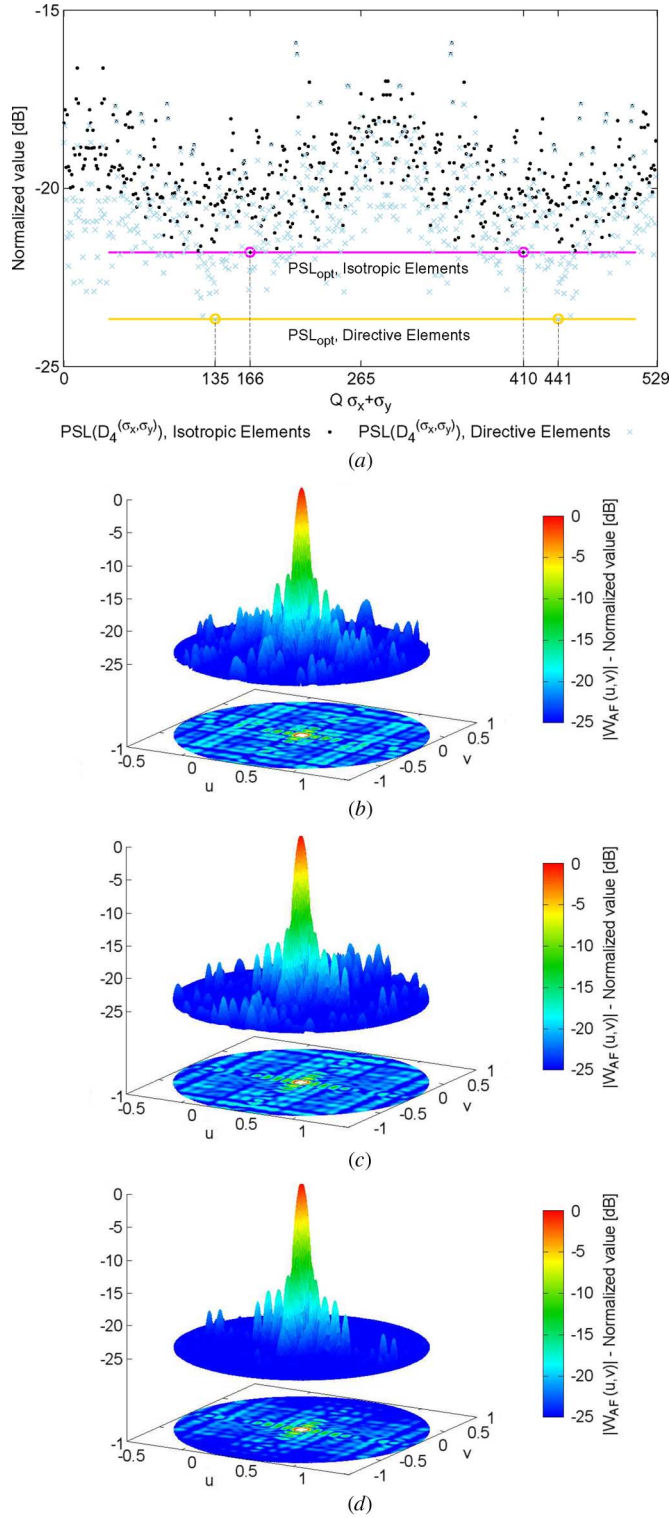


Fig. 11. *Numerical Validation—Non-Isotropic elements.* PSL values of the ADS-based arrays generated from the sequences  $\underline{D}_4^{(\sigma_x, \sigma_y)}$ ,  $\sigma_x = 0, \dots, P-1$ ,  $\sigma_y = 0, \dots, Q-1$  (a). Normalized array patterns of the arrays generated from the sequences (b)  $\underline{D}_4^{\text{opt}} = \underline{D}_4^{(7,5)}$  with isotropic elements,  $\underline{D}_4^{(5,20)}$  with isotropic (c) and directive elements (d).

- because of the three-level autocorrelation function, ADS sequences guarantee additional degrees-of-freedom (compared to the DS case) to be profitably exploited (e.g., using directive elements) for fitting the design constraints;

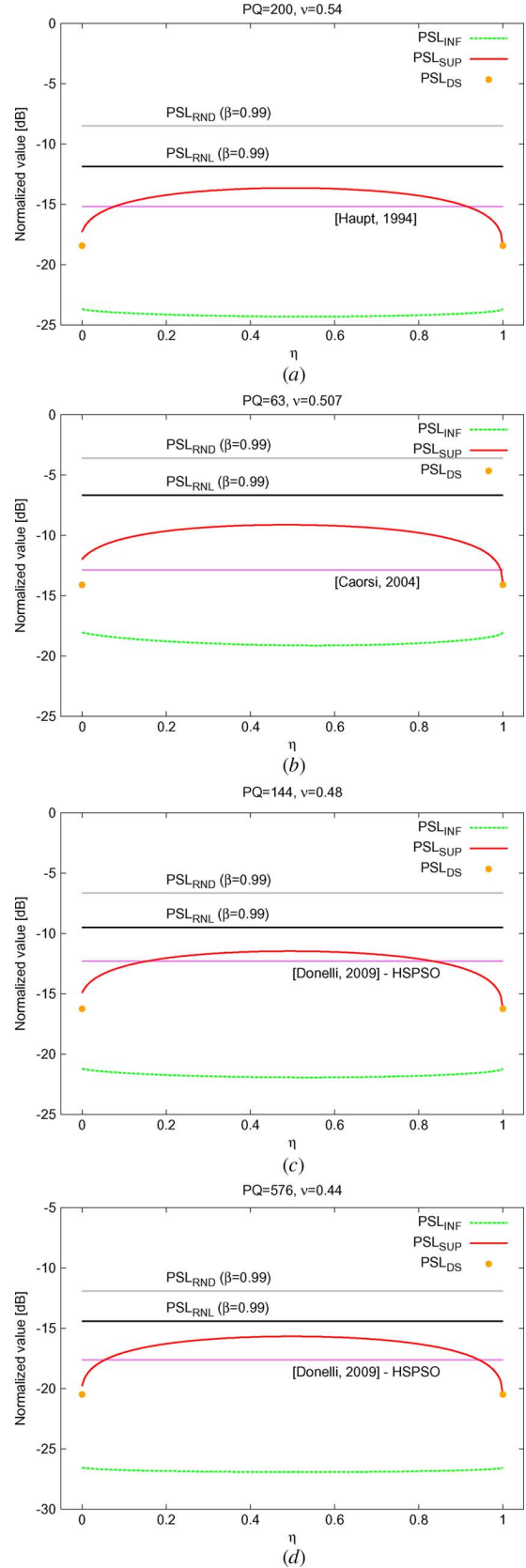


Fig. 12. *Comparative Assessment.* Plots of the PSL bounds versus the array aperture,  $PQ$ , when  $\eta = 0.5$  and for (a)  $\nu = 0.54$  [5], (b)  $\nu = 0.507$  [7], (c)  $\nu = 0.48$  [18], (d)  $\nu = 0.44$  [18].

- unlike iterative optimization or trial-and-test random synthesis techniques, the approach determines the array con-

figuration just through simple shifts of a reference ADS sequence;

- thanks to the availability of rich repositories of ADSs also concerned with large  $P$  and  $Q$  indexes, wide apertures (impracticable for stochastic optimizers) can be dealt with;
- the use of ADS does not prevent their integration with optimization techniques, vice versa it could represent a way (to be explored in successive researches) to improve the convergence rate of iterative methods or for enabling stochastic searches in thinning large arrays by means of a suitable ADS-based initialization.

In addition to these features, other main contributions of the present paper consist in the following methodological novelties:

- 1) an innovative and compact analytic formulation for the analysis of the PSL based on the relations between the DTFT and the DFT of ADS binary sequences that avoids the exploitation of the “infinite array” formalism [6], [27] generally more complicated when dealing with planar arrangements;
- 2) unlike ADS-based linear arrays [27], the exploitation of the information on  $\min_{(k,l) \in \mathcal{H}_0} \{|\mathbb{F}^{(\sigma_x, \sigma_y)}(k, l)|^2\}$  to derive a more tight  $\text{PSL}_{\min}$  bound for planar geometries.

Future works will be devoted to further extend the proposed analysis to other geometries and problems. Moreover, although out-of-the-scope of the present paper since not pertinent to antenna arrays but concerned with combinatorial mathematics, other advances in the research activities concerned with the explicit determination of other ADS sequences are certainly expected.

#### APPENDIX

*Definition of the Mainlobe Region  $R$ :* Starting from (12) as for planar DS arrays [6], it can be proved that the PSL of ADS-based arrays is close to the values of the samples of the array factor at  $u = u_{m+(1/2)} \triangleq (m + 1/2)/Px_0$ ,  $v = v_{n+(1/2)} \triangleq$

$(n + 1/2)/Qy_0$ . By exploiting such an observation, one can obtain (17), shown at the bottom of the page, where the mainlobe region,  $R$ , is defined analogously to [6] as the visible region where the first term in (17) exceeds the magnitude of the second one. As regards the first term, its magnitude is approximately equal to

$$\frac{K}{\pi^2 \left(m + \frac{1}{2}\right) \left(n + \frac{1}{2}\right)}$$

and for large values of  $P$  and  $Q$ . Moreover, the largest coefficients in the second term (i.e.,  $m + k + (1/2) = \pm 1$  and  $n + l + (1/2) = \pm 1$ ) of (17) are bounded by

$$\frac{4 \max_{(k,l) \in \mathcal{H}_0} |\mathbb{F}^{(\sigma_x, \sigma_y)}|}{\pi^2}.$$

Thus, after simple manipulation, it is possible to show that  $R$  extends to the region limited by the following boundary inequality

$$u_{m+\frac{1}{2}} v_{n+\frac{1}{2}} \leq \frac{K}{4PQx_0y_0 \max_{(k,l) \in \mathcal{H}_0} |\mathbb{F}^{(\sigma_x, \sigma_y)}|}. \quad (18)$$

*Derivation of  $\text{PSL}_{\text{SUP}}$  in (13):* With reference to discrete version of  $R$ ,  $R_D$ ,

$$R_D \triangleq \left\{ (m, n) \in \mathbb{Z} \times \mathbb{Z} : \left( m + \frac{1}{2} \right) \left( n + \frac{1}{2} \right) \leq \frac{K}{4 \max_{(k,l) \in \mathcal{H}_0} |W_{\text{DFT}}(k, l)|} \right\} \quad (19)$$

let us consider the following approximation of  $\text{PSL}^{\text{opt}}\{\mathbf{D}\} = \min_{(\sigma_x, \sigma_y)} [\text{PSL}\{\mathbf{D}^{(\sigma_x, \sigma_y)}\}]$ , shown in (20) at the bottom of the page, where the complex coefficient  $\mathbb{F}^{(\sigma_x, \sigma_y)}$  has been expressed in terms of its amplitude,  $\sqrt{|\mathbb{F}^{(\sigma_x, \sigma_y)}(k, l)|^2}$ , and phase,  $\phi_{kl}^{(\sigma_x, \sigma_y)}$ .

$$\text{PSL}\{\mathbf{D}^{(\sigma_x, \sigma_y)}\} \approx \frac{1}{K^2} \times \max_{\left(u_{m+\frac{1}{2}}, v_{n+\frac{1}{2}}\right) \notin R} \left| \frac{K(-1)^{m+n}}{PQ \sin\left[\frac{\pi}{P}\left(m + \frac{1}{2}\right)\right] \sin\left[\frac{\pi}{Q}\left(n + \frac{1}{2}\right)\right]} + \sum_{k=0, k \neq 0}^{P-1} \sum_{l=0, l \neq 0}^{Q-1} \frac{\mathbb{F}^{(\sigma_x, \sigma_y)}(-1)^{m+k+n+l}}{PQ \sin\left[\frac{\pi}{P}\left(m + k + \frac{1}{2}\right)\right] \sin\left[\frac{\pi}{Q}\left(n + l + \frac{1}{2}\right)\right]} \right|^2 \quad (17)$$

$$\text{PSL}^{\text{opt}}\{\mathbf{D}\} \lesssim \min_{(\sigma_x, \sigma_y)} \left[ \frac{\max_{(k,l) \in \mathcal{H}_0} \{|\mathbb{F}^{(\sigma_x, \sigma_y)}(k, l)|^2\}}{K^2} \times \max_{(m,n) \notin R_D} \left| \sum_{k=0, k \neq 0}^{P-1} \sum_{l=0, l \neq 0}^{Q-1} \frac{e^{j\phi_{kl}^{(\sigma_x, \sigma_y)}}(-1)^{m+k+n+l}}{PQ \sin\left[\frac{\pi}{P}\left(m + k + \frac{1}{2}\right)\right] \sin\left[\frac{\pi}{Q}\left(n + l + \frac{1}{2}\right)\right]} \right|^2 \right] \quad (20)$$

It is worth pointing out that, likewise DSs,  $\phi_{kl}^{(\sigma_x, \sigma_y)}$  is not *a-priori* known as well as, unlike DSs, the term  $\max_{(k,l) \in \mathcal{H}_0} \{|\mathbb{F}^{(\sigma_x, \sigma_y)}(k, l)|^2\}$  and they have to be estimated. Towards this end, by exploiting the circular correlation property of DFT [30], it is possible to state that

$$\begin{aligned} |\mathbb{F}^{(\sigma_x, \sigma_y)}(k, l)|^2 &= \text{DFT} \{A_w^{\text{ADS}}(p, q)\} \\ &= K - \Lambda + PQ\Lambda\delta(k, l) + \Psi(k, l) \end{aligned} \quad (21)$$

and to obtain the following relationship

$$\max_{(k,l) \in \mathcal{H}_0} \left\{ |\mathbb{F}^{(\sigma_x, \sigma_y)}(k, l)|^2 \right\} = K - \Lambda + \max_{(k,l) \in \mathcal{H}_0} \{ \Psi(k, l) \} \quad (22)$$

where  $\Psi(k, l) \triangleq \text{DFT} \{ \psi(p, q) \}$  being  $\psi(p, q) \triangleq \sum_{r=1}^{PQ-1-t} \delta(p - l_{r,1}, q - l_{r,2})$ .

Concerning the real-valued coefficients  $\Psi(k, l)$ , by applying the Parseval's theorem [30]

$$\frac{1}{PQ} \sum_{k=0}^{P-1} \sum_{l=0}^{Q-1} |\Psi(k, l)|^2 = \sum_{p=0}^{P-1} \sum_{q=0}^{Q-1} |\psi(p, q)|^2 = PQ - 1 - t,$$

and noticing that  $\sum_{p=0}^{P-1} \sum_{q=0}^{Q-1} |\psi(p, q)|^2 = PQ - 1 - t$  and  $\Psi(0, 0) = PQ - 1 - t$ , the following holds true

$$\sum_{k=0, kl \neq 0}^{P-1} \sum_{l=0, kl \neq 0}^{Q-1} |\Psi(k, l)|^2 = (t+1)(PQ - 1 - t). \quad (23)$$

Therefore, since

$$\begin{aligned} \max_{(k,l) \in \mathcal{H}_0} \{ \Psi(k, l) \} &\leq \max_{(k,l) \in \mathcal{H}_0} \{ |\Psi(k, l)| \} \\ &\leq \sqrt{(t+1)(PQ - 1 - t)} \end{aligned} \quad (24)$$

and substituting (22) in (20), we obtain (25) at the bottom of the page.

As regards the phase terms  $\phi_{kl}^{(\sigma_x, \sigma_y)}$ , the analysis is carried out as in [6] in order to give an estimate of the PSL. More specifically, although the phase terms  $\phi_{kl}^{(\sigma_x, \sigma_y)}$  are deterministic quantities, they are dealt with as independent identically distributed (i.i.d.) uniform random variables. Under this assumption, (25) can be expressed as

$$\text{PSL}^{\text{opt}} \{ \mathbf{D} \} \lesssim \frac{(K - \Lambda + \sqrt{(t+1)(PQ - 1 - t)}) \Gamma^{\text{opt}}}{K^2} \quad (26)$$

where for large  $P$  and  $Q$

$$\Gamma^{\text{opt}} \approx \min_{(\sigma_x, \sigma_y)} \{ \max[U_i; i = 1, \dots, \Pi] \} \quad (27)$$

$U_i \triangleq |\sum_{k=-\infty}^{\infty} \sum_{l=-\infty}^{\infty} (e^{j\phi_{kl}^{(\sigma_x, \sigma_y)}} / \pi^2 (k + (1/2))(l + (1/2)))|^2$ ,  $i = 1, \dots, \Pi$ , being i.i.d. random variables and  $\Pi$  is the cardinality of  $R_D (\approx PQ)$ . Since the statistics of  $\Gamma^{\text{opt}}$  are not available in closed form, Monte Carlo simulations have been performed to provide an approximation of its mean value  $E\{\Gamma^{\text{opt}}\}$

$$E\{\Gamma^{\text{opt}}\} \approx -0.1 + 1.5 \log_{10}(PQ). \quad (28)$$

By substituting (28) in (26), the upper bound  $\text{PSL}_{\text{SUP}}$  is finally obtained.

*Derivation of  $\text{PSL}_{\text{INF}}$  in (13):* By sampling (12) at  $(u = s/Pd_x, v = t/Qd_y)$ ,  $s = 0, \dots, P-1$ ,  $t = 0, \dots, Q-1$ , one can obtain (29), shown at the bottom of the page.

By substituting (22) in (29), and observing that

$$\max_{(k,l) \in \mathcal{H}_0} \{ \Psi(k, l) \} \geq -\sqrt{\frac{(t+1)(PQ - 1 - t)}{PQ - 1}} \quad (30)$$

it turns out

$$\text{PSL}^{\text{opt}} \{ \mathbf{D} \} \geq \frac{K - \Lambda - \sqrt{\frac{(t+1)(PQ - 1 - t)}{PQ - 1}}}{K^2} \triangleq \text{PSL}_{\text{INF}}. \quad (31)$$

---


$$\begin{aligned} \text{PSL}^{\text{opt}} \{ \mathbf{D} \} &\lesssim \frac{(K - \Lambda + \sqrt{(t+1)(PQ - 1 - t)})}{K^2} \\ &\quad \times \min_{(\sigma_x, \sigma_y)} \left[ \max_{(m,n) \notin R_D} \left| \sum_{k=0, kl \neq 0}^{P-1} \sum_{l=0, kl \neq 0}^{Q-1} \frac{e^{j\phi_{kl}^{(\sigma_x, \sigma_y)}} (-1)^{m+k+n+l}}{PQ \sin \left[ \frac{\pi}{P} (m + k + \frac{1}{2}) \right] \sin \left[ \frac{\pi}{Q} (n + l + \frac{1}{2}) \right]} \right|^2 \right]. \end{aligned} \quad (25)$$


---

$$\begin{aligned} \text{PSL}^{\text{opt}} \{ \mathbf{D} \} &\geq \text{PSL} \left\{ \mathbf{D}^{(\sigma_x, \sigma_y)} \right\} \Big|_{u=\frac{s}{Pd_x}, v=\frac{t}{Qd_y}} \\ &= \frac{\max_{(s,t) \in \mathcal{H}_0} \left| \sum_{k=0}^{P-1} \sum_{l=0}^{Q-1} \mathbb{F}^{(\sigma_x, \sigma_y)}(k, l) \mathcal{S}_P \left[ \frac{\pi(s+k)}{P} \right] \mathcal{S}_Q \left[ \frac{\pi(t+l)}{Q} \right] \right|^2}{K^2} \\ &= \frac{\max_{(s,t) \in \mathcal{H}_0} |\mathbb{F}^{(\sigma_x, \sigma_y)}(s, t)|^2}{K^2}. \end{aligned} \quad (29)$$

*Derivation of  $PSL_{max}$  in (13):* With reference to (20), let us assume that the ADS  $\underline{\mathbf{D}}$  at hand is known. Thus,

$$\Omega\{\underline{\mathbf{D}}\} \triangleq \max_{(k,l) \in \mathcal{H}_0} \left| \mathbb{F}^{(\sigma_x, \sigma_y)}(k, l) \right|^2 \quad (32)$$

is now a known quantity. By substituting (32) in (20), we obtain (33), shown at the bottom of the page.

As regards the phase terms  $\phi_{kl}^{(\sigma_x, \sigma_y)}$ , let us consider the same procedure used for deriving  $PSL_{SUP}$  and let us rewrite (33) as follows:

$$PSL^{\text{opt}}\{\underline{\mathbf{D}}\} \lesssim \frac{\Omega\{\underline{\mathbf{D}}\} \Gamma^{\text{opt}}}{K^2} \quad (34)$$

where  $\Gamma^{\text{opt}}$  is successively approximated with its mean value (28) to obtain  $PSL_{max}$ .

*Derivation of  $PSL_{min}$  in (13):* Let us start from (17), and consider the following approximation of  $PSL^{\text{opt}}\{\underline{\mathbf{D}}\}$ , see (35) shown at the bottom of the page.

By using (19) and expressing the complex coefficients  $\mathbb{F}^{(\sigma_x, \sigma_y)}$  in terms of their amplitude and phase, we can approximate (35) as follows in (36), shown at the bottom of the page.

In order to provide a lower bound to such an expression, let us observe that the following equation holds true (see (37) at the bottom of the page).

The two terms on the right-hand side of (37) are then treated separately. As regards the first factor, it can be observed that, when the ADS sequence is explicitly available, it is a known quantity equal to

$$\Xi\{\underline{\mathbf{D}}\} \triangleq \min_{(k,l) \in \mathcal{H}_0} \left| \mathbb{F}^{(\sigma_x, \sigma_y)}(k, l) \right|^2. \quad (38)$$

Therefore, by substituting (38) in (37), we obtain (39), shown at the top of the next page.

As for the second term, an analysis similar to that carried out for deriving  $PSL_{SUP}$  is still possible. However, the two summations cannot be extended here up to  $\pm\infty$  as in (27). Indeed,

---


$$PSL^{\text{opt}}\{\underline{\mathbf{D}}\} \lesssim \frac{\Omega\{\underline{\mathbf{D}}\}}{K^2} \min_{(\sigma_x, \sigma_y)} \left[ \max_{(m,n) \notin R_D} \left| \sum_{k=0, kl \neq 0}^{P-1} \sum_{l=0, kl \neq 0}^{Q-1} \frac{e^{j\phi_{kl}^{(\sigma_x, \sigma_y)}} (-1)^{m+k+n+l}}{PQ \sin \left[ \frac{\pi}{P} \left( m + k + \frac{1}{2} \right) \right] \sin \left[ \frac{\pi}{Q} \left( n + l + \frac{1}{2} \right) \right]} \right|^2 \right] \quad (33)$$


---

$$PSL^{\text{opt}}\{\underline{\mathbf{D}}\} \approx \min_{(\sigma_x, \sigma_y)} \left\{ \frac{1}{K^2} \max_{\left( u_{m+\frac{1}{2}}, v_{n+\frac{1}{2}} \right) \notin R} \left| \frac{K(-1)^{m+n}}{PQ \sin \left[ \frac{\pi}{P} \left( m + \frac{1}{2} \right) \right] \sin \left[ \frac{\pi}{Q} \left( n + \frac{1}{2} \right) \right]} + \sum_{k=0, kl \neq 0}^{P-1} \sum_{l=0, kl \neq 0}^{Q-1} \frac{\mathbb{F}^{(\sigma_x, \sigma_y)}(k, l) (-1)^{m+k+n+l}}{PQ \sin \left[ \frac{\pi}{P} \left( m + k + \frac{1}{2} \right) \right] \sin \left[ \frac{\pi}{Q} \left( n + l + \frac{1}{2} \right) \right]} \right|^2 \right\}. \quad (35)$$


---

$$PSL^{\text{opt}}\{\underline{\mathbf{D}}\} \approx \frac{1}{K^2} \min_{(\sigma_x, \sigma_y)} \left\{ \max_{(m,n) \notin R_D} \left| \sum_{k=0, kl \neq 0}^{P-1} \sum_{l=0, kl \neq 0}^{Q-1} \frac{|\mathbb{F}^{(\sigma_x, \sigma_y)}(k, l)| e^{\phi_{kl}^{(\sigma_x, \sigma_y)}} (-1)^{m+k+n+l}}{PQ \sin \left[ \frac{\pi}{P} \left( m + k + \frac{1}{2} \right) \right] \sin \left[ \frac{\pi}{Q} \left( n + l + \frac{1}{2} \right) \right]} \right|^2 \right\} \quad (36)$$


---

$$PSL^{\text{opt}}\{\underline{\mathbf{D}}\} \gtrsim \min_{(\sigma_x, \sigma_y)} \left\{ \frac{\min_{(k,l) \in \mathcal{H}_0} |\mathbb{F}^{(\sigma_x, \sigma_y)}(k, l)|^2}{K^2} \times \max_{(m,n) \notin R_D} \left| \sum_{k=0, kl \neq 0}^{P-1} \sum_{l=0, kl \neq 0}^{Q-1} \frac{e^{\phi_{kl}^{(\sigma_x, \sigma_y)}} (-1)^{m+k+n+l}}{PQ \sin \left[ \frac{\pi}{P} \left( m + k + \frac{1}{2} \right) \right] \sin \left[ \frac{\pi}{Q} \left( n + l + \frac{1}{2} \right) \right]} \right|^2 \right\}. \quad (37)$$



$$\text{PSL}^{\text{opt}}\{\mathbf{D}\} \approx \frac{\Xi\{\mathbf{D}\}}{K^2} \min_{(\sigma_x, \sigma_y)} \left\{ \max_{(m,n) \notin R_D} \left| \sum_{k=0, kl \neq 0}^{P-1} \sum_{l=0, kl \neq 0}^{Q-1} \frac{e^{\phi_{kl}^{(\sigma_x, \sigma_y)}} (-1)^{m+k+n+l}}{PQ \sin\left[\frac{\pi}{P}\left(m+k+\frac{1}{2}\right)\right] \sin\left[\frac{\pi}{Q}\left(n+l+\frac{1}{2}\right)\right]} \right|^2 \right\}. \quad (39)$$

$$\min_{(\sigma_x, \sigma_y)} \left\{ \max_{(m,n) \notin R_D} \left| \sum_{k=0, kl \neq 0}^{P-1} \sum_{l=0, kl \neq 0}^{Q-1} \frac{e^{\phi_{kl}^{(\sigma_x, \sigma_y)}} (-1)^{m+k+n+l}}{PQ \sin\left[\frac{\pi}{P}\left(m+k+\frac{1}{2}\right)\right] \sin\left[\frac{\pi}{Q}\left(n+l+\frac{1}{2}\right)\right]} \right|^2 \right\} \approx 0.5 + 0.8 \log_{10}(PQ). \quad (40)$$

by performing a Monte Carlo analysis, it turns out that the approximation (see (40) at the top of the page) holds true for large values of  $P \times Q$ , which, substituted in (39), provides the lower bound  $\text{PSL}_{\min}$ .

#### ACKNOWLEDGMENT

A. Massa wishes to thank E. Vico for being and C. Pedrazzani for her continuous help and patience. Moreover, the authors are very grateful to M. Donelli for kindly providing some numerical results of computer simulations. Furthermore, the authors greatly appreciated the reviewing and valuable comments of the anonymous reviewers of a previously submitted version of the manuscript.

#### REFERENCES

- [1] C. A. Balanis, *Antenna Theory: Analysis and Design*, 2nd ed. New York: Wiley, 1997.
- [2] Y. T. Lo, "A mathematical theory of antenna arrays with randomly spaced elements," *IEEE Trans. Antennas Propag.*, vol. 12, no. 3, pp. 257–268, May 1964.
- [3] B. Steinberg, "The peak sidelobe of the phased array having randomly located elements," *IEEE Trans. Antennas Propag.*, vol. 20, no. 2, pp. 129–136, Mar. 1972.
- [4] D. G. Leeper, "Thinned periodic antenna arrays with improved peak sidelobe level control," U.S. Patent 4071848, Jan. 31, 1978.
- [5] R. L. Haupt, "Thinned arrays using genetic algorithms," *IEEE Trans. Antennas Propag.*, vol. 42, no. 7, pp. 993–999, Jul. 1994.
- [6] D. G. Leeper, "Isophoric arrays—Massively thinned phased arrays with well-controlled sidelobes," *IEEE Trans. Antennas Propag.*, vol. 47, no. 12, pp. 1825–1835, Dec. 1999.
- [7] S. Caorsi, A. Lommi, A. Massa, and M. Pastorino, "Peak sidelobe reduction with a hybrid approach based on GAs and difference sets," *IEEE Trans. Antennas Propag.*, vol. 52, no. 4, pp. 1116–1121, Apr. 2004.
- [8] R. L. Haupt and D. H. Werner, *Genetic Algorithms in Electromagnetics*. Hoboken, NJ: Wiley, 2007.
- [9] B. Steinberg, "Comparison between the peak sidelobe of the random array and algorithmically designed aperiodic arrays," *IEEE Trans. Antennas Propag.*, vol. 21, no. 3, pp. 366–370, May 1973.
- [10] M. I. Skolnik, G. Nemhauser, and J. W. Sherman, III, "Dynamic programming applied to unequally-spaced arrays," *IRE Trans. Antennas Propag.*, vol. AP-12, pp. 35–43, Jan. 1964.
- [11] S. Holm, B. Elgetun, and G. Dahl, "Properties of the beam pattern of weight- and layout-optimized sparse arrays," *IEEE Trans. Ultrason., Ferroelectr., Freq. Control*, vol. 44, no. 5, pp. 983–991, Sep. 1997.
- [12] T. G. Spence and D. H. Werner, "Thinning of aperiodic antenna arrays for low side-lobe levels and broadband operation using genetic algorithms," in *Proc. IEEE Antennas and Propagation Society Int. Symp.*, Jul. 9–14, 2006, pp. 2059–2062.
- [13] C. S. Ruf, "Numerical annealing of low-redundancy linear arrays," *IEEE Trans. Antennas Propag.*, vol. 41, no. 1, pp. 85–90, Jan. 1993.
- [14] V. Murino, A. Trucco, and C. S. Regazzoni, "Synthesis of unequally spaced arrays by simulated annealing," *IEEE Trans. Signal Processing*, vol. 44, no. 1, pp. 119–123, Jan. 1996.
- [15] M. Vicente-Lozano, F. Ares, and E. Moreno, "Pencil-beam pattern synthesis with a uniformly excited multi-ring planar antenna," *IEEE Antennas Propag. Mag.*, vol. 42, no. 6, pp. 70–74, Dec. 2000.
- [16] F. Ares, J. Fondevila-Gomez, G. Franceschetti, E. Moreno-Piquero, and J. A. Rodriguez-Gonzalez, "Synthesis of very large planar arrays for prescribed footprint illumination," *IEEE Trans. Antennas Propag.*, vol. 56, no. 2, pp. 584–589, Feb. 2008.
- [17] M. Alvarez-Folgueiras, J. A. Rodriguez-Gonzalez, and F. Ares, "Low-sidelobe patterns from small, low-loss uniformly fed linear arrays illuminating parasitic dipoles," *IEEE Trans. Antennas Propag.*, vol. 57, no. 5, pp. 1584–1586, May 2009.
- [18] M. Donelli, A. Martini, and A. Massa, "A hybrid approach based on PSO and Hadamard difference sets for the synthesis of square thinned arrays," *IEEE Trans. Antennas Propag.*, vol. 57, no. 8, pp. 2491–2495, Aug. 2009.
- [19] L. E. Kopilovich and L. G. Sodin, "Two-dimensional aperiodic antenna arrays with a low sidelobe level," *Proc. Inst. Elect. Eng.*, vol. H-138, no. 3, pp. 233–237, 1991.
- [20] L. E. Kopilovich and L. G. Sodin, "Synthesis of two-dimensional non-equidistant antenna arrays on the basis of difference set theory," *J. Commun. Technol. Electron.*, vol. 39, pp. 33–42, 1994.
- [21] L. E. Kopilovich and L. G. Sodin, *Multielement System Design in Astronomy and Radio Science*. Dordrecht/Boston/London: Kluwer Academic Publishers, Astrophysics and Space Science Library, 2001, vol. 268.
- [22] L. E. Kopilovich, "Square array antennas based on hadamard difference sets," *IEEE Trans. Antennas Propag.*, vol. 56, no. 1, pp. 263–266, Jan. 2008.
- [23] La Jolla Cyclic Difference Set Repository [Online]. Available: <http://www.ccrwest.org/diffsets.html>
- [24] C. Ding, T. Hellesteth, and K. Y. Lam, "Several classes of binary sequences with three-level autocorrelation," *IEEE Trans. Inf. Theory*, vol. 45, no. 7, pp. 2606–2612, Nov. 1999.
- [25] K. T. Arasu, C. Ding, T. Hellesteth, P. V. Kumar, and H. M. Martinsen, "Almost difference sets and their sequences with optimal autocorrelation," *IEEE Trans. Inf. Theory*, vol. 47, no. 7, pp. 2934–2943, Nov. 2001.
- [26] Y. Zhang, J. G. Lei, and S. P. Zhang, "A new family of almost difference sets and some necessary conditions," *IEEE Trans. Inf. Theory*, vol. 52, no. 5, pp. 2052–2061, May 2006.
- [27] G. Oliveri, M. Donelli, and A. Massa, "Linear array thinning exploiting almost difference sets," *IEEE Trans. Antennas Propag.*, vol. 57, no. 12, pp. 3800–3812, Dec. 2009.
- [28] ELEDIA Almost Difference Set Repository [Online]. Available: <http://www.ing.unitn.it/~eledia/html/>
- [29] M. I. Kargapolov and J. I. Merzljako, *Fundamentals of the Theory of Groups*. New York: Springer-Verlag, 1979.
- [30] J. G. Proakis and D. G. Manolakis, *Digital Signal Processing: Principles, Algorithms, and Applications*, 3rd ed. London: Prentice Hall, 1996.



**Giacomo Oliveri** (M'09) received the "Laurea" degree in telecommunications engineering and the Ph.D. degree in space science and engineering from the University of Genoa, Italy, in 2005 and 2009, respectively.

He is a member of the ELEDIA Research Group, University of Trento, Italy. His main research is focused on antenna arrays, electromagnetic propagation in complex environments and numerical methods for electromagnetic problems.



**Luca Manica** (S'09) was born in Rovereto, Italy. He received the B.S. and M.S. degrees in telecommunication engineering both from University of Trento, Italy, in 2004 and 2006, respectively, where he is currently working toward the Ph.D. degree.

He is a member of the ELEDIA Research Group, University of Trento, Italy. His main interests are the synthesis of the antenna array patterns and fractal antennas.



**Andrea Massa** (M'03) received the "Laurea" degree in electronic engineering and the Ph.D. degree in electronics and computer science from the University of Genoa, Genoa, Italy, in 1992 and 1996, respectively.

From 1997 to 1999, he was an Assistant Professor of Electromagnetic Fields at the Department of Biophysical and Electronic Engineering (University of Genoa) teaching the university course of Electromagnetic Fields 1. From 2001 to 2004, he was an Associate Professor at the University of Trento.

Since 2005, he has been a Full Professor of Electromagnetic Fields at the University of Trento, where he currently teaches electromagnetic fields, inverse scattering techniques, antennas and wireless communications, and optimization techniques. At present, he is the Director of the ELEDIALab at the University of Trento and Deputy Dean of the Faculty of Engineering. His research work since 1992 has been principally on electromagnetic direct and inverse scattering, microwave imaging, optimization techniques, wave propagation in presence of nonlinear media, wireless communications and applications of electromagnetic fields to telecommunications, medicine and biology.

Prof. Massa is a member of the IEEE Society, of the PIERS Technical Committee, of the Inter-University Research Center for Interactions Between Electromagnetic Fields and Biological Systems (ICEmB) and Italian representative in the general assembly of the European Microwave Association (EuMA).